Sakarya University Journal of Science

ISSN : 2147-835X
Publisher : Sakarya University

Vol. 28, No. 3, 466-479, 2024
DOI: https://doi.org/10.16984/saufenbilder.1211242

Research Article

An Approach for Modelling Accidental Eccentricity Effects in Symmetrical Frame Buildings Exhibiting Semi-Rigid Diaphragm Behavior

Melih Sürmeli

Bursa Technical University, Faculty of Engineering and Natural Sciences, Department of Civil Engineering, Bursa, Türkiye, melih.surmeli@btu.edu.tr

ARTICLE INFO

Keywords:
Accidental eccentricity
Semi-rigid diaphragm
Flexible diaphragm
Precast building
RC building

Article History:
Received: 28.11.2022
Accepted: 18.03.2024
Online Available: 06.06.2024

ABSTRACT

The accidental eccentricity effect is specified, in earthquake codes, to account for the possible uncertainties in the mass and stiffness distribution of the structural system and the effect of the torsional component of the earthquake ground motion on the building. Türkiye Building Earthquake Code (TBEC-2018) considers the additional eccentricity effect only for the cases where rigid diaphragm behavior is provided in the slabs. However, in buildings with A2 and A3 irregularities or flexible diaphragms including insufficient strength and stiffness, the in-plane deformations and stresses on diaphragms may change the behavior of buildings under earthquake loads.
In this study, a practical approach to be used in the equivalent earthquake load method was proposed to apply the accidental eccentricity effect on symmetrical frame buildings with semi-rigid diaphragms. The approach is based on distributing the total accidental torsion to the nodes as fictitious forces. Two numerical examples were presented. The first is a single-story precast industrial-type RC building, where the calculation steps of the procedure explained in detail. The building was modeled with both semi-rigid and rigid diaphragm assumptions, and a comparison of two modeling assumptions under accidental torsion was presented. Torsional irregularity factors obtained from building modeled by semi-rigid diaphragm assumption provided greater values with respect to those modeled by rigid diaphragm. This shows the significance of considering accidental eccentricity for semi-rigid diaphragms. The second numerical example, which is a RC concrete building, was used to validate the proposed methodology via finite element model (FEM) built-in algorithm. The obtained displacement demands by using the proposed methodology were very close to FEM results as a reference for the real solution. It is concluded from this study that the proposed methodology is reliable and can be used for modeling accidental eccentricity effects on symmetrical-plan buildings with semi-rigid diaphragms.

1. Introduction

In addition to carrying vertical loads, another important task of flooring and roofing systems is to transfer the inertia forces to the foundation safely under horizontal loads. In this context, the degree of flexibility of the diaphragms plays an important role. ASCE 7.16 [1] Chapter 12.3.1 classifies diaphragms as rigid and flexible. If horizontal loads are distributed to vertical elements in proportion to their relative stiffness under earthquake loads and the in-plane deformation of the diaphragm is negligible, the diaphragm is classified as rigid. Both inherent and accidental torsion should be included in the analysis model in the case of a rigid diaphragm. Therefore, the flexural stiffness of all vertical elements for two orthogonal earthquake directions, and beams' flexural stiffnesses with respect to diaphragm plane should be found in the mathematical model. The greater horizontal stiffness of the rigid diaphragm results in smaller period values than the flexible diaphragm, leading to larger earthquake forces being transferred to vertical elements.

Cite as: M. Sürmeli (2024). An Approach for Modelling Accidental Eccentricity Effects in Symmetrical Frame Buildings Exhibiting Semi-Rigid Diaphragm Behavior, *Sakarya University Journal of Science*, 28(3), 466-479. https://doi.org/10.16984/saufenbilder.1211242

In accordance with ASCE 7.16, flexible diaphragm is defined based on two criteria. The first one is classified as prescriptive criteria, which is not applicable to RC precast buildings directly. The latter criteria, referred as calculated criteria, is expressed such that in-plane deflection under lateral load is more than two times the average story drift of the adjoining vertical elements. Figure 1 illustrates the deflections of flexible diaphragm. Deflection δ_{MDD} is the mid-span deflection of the flexible diaphragm and δ_{ADVE} is the average deflection of vertical elements.

Therefore, the flexible diaphragm condition can be defined as $\delta_{MDD}/\ \delta_{ADVE} > 2$. The lateral loads are distributed to the supporting vertical elements via the beams reflecting in-plane stiffness of flexible diaphragm. Hence, the distribution of horizontal forces to vertical elements is independent of their relative stiffness. Instead, the inertia forces are proportional to masses corresponding to tributary areas of each vertical element. Therefore, a two-dimensional beam model with supporting vertical elements can be sufficient to analyze the flexible diaphragm under horizontal loads for single-story buildings, and the vertical elements are designed based on the tributary masses assigned. For multi-story buildings, each frame may be modeled independently, with seismic masses assigned to tributary area. Such type of behavior of flexible diaphragms prevents the efficient transmission of torsional forces to vertical elements.

In fact, the diaphragms behave neither rigid nor flexible, the behavior is between two cases, in other words, semi-rigidly. Related to this subject, ASCE 7-16 Section 12.3.1 states that the stiffness of the diaphragm should be included in the model. In certain circumstances such as the buildings having plan irregularities etc., TBDY-2018 necessitates modeling the buildings with both rigid and semi-rigid diaphragms. For the model with a rigid diaphragm, the accidental eccentricity effects are taken into consideration. This modeling assumption is mostly used for the design of vertical elements. While, semi-rigid modeling assumption without considering accidental eccentricity is used to determine design forces for all structural elements, and slabs are designed according to this. The envelope of the two modeling assumptions then is selected as the final design case. As a more realistic approach, the building may be modeled with semi-rigid diaphragm considering accidental eccentricity effects. Thus, both flexibility of the diaphragm and the flexibility of vertical elements are taken into account including accidental and inherent torsion in the design. In this context, the stiffness of the roof and slab members should be carefully modeled. ASCE 7.16 C12.8.4.2 states that accidental torsional moment can be defined as the summation of nodal moments or forces through the diaphragm.

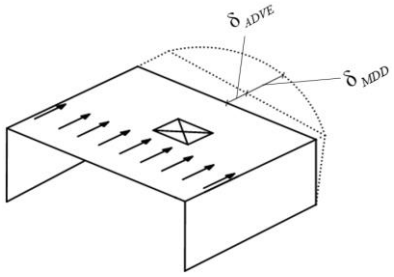

Figure 1. Flexible diaphragm [1]

Several researches about the flexibility of horizontal diaphragms have been conducted in recent years [2-13]. In general, the degree of flexibility of diaphragms have been investigated via nonlinear time history analysis for buildings with rigid perimeter shear walls or vertical trusses. It has been found as a common result that the fundamental periods of the buildings considering flexible diaphragms are greater than those modeled by rigid diaphragms. This can result from a smaller base shear value if one design the building with the rigid diaphragm. The degree of flexibility increases as the depth-to-length ratio of diaphragm increases.

Mortazawi and Humar [2], Humar and Popovski [3] investigated the effects of flexibility on the ductility demand and internal forces in the diaphragm. They concluded that flexibility caused a significant increase in the ductility demand on the lateral load-resisting system, particularly when the diaphragm is designed to remain elastic. Also, a significant increase in bending moment at mid-span and shear force at the quarter span of diaphragm were observed. Sadashiva et al. [4, 5] showed that the diaphragm flexibility mostly affects single-story structures, and reported that an increase in the number of

stories decreases the diaphragm flexibility. Shake table tests were performed by Tremblay et al. [6] to investigate the behavior of low-rise steel buildings with flexible roof diaphragms including metal roof deck diaphragms. Shrestha [7] conducted a study to investigate the flexibility and ductility characteristics of steel deck roof diaphragms and to incorporate this information into the design of single-story steel buildings.

The numerical analysis was performed by Opensees using trusses for metal roof decks. Farrow and Fleischman [8, 9] investigated the expected seismic demands for precast concrete parking structure diaphragms and proposed seismic design guidelines for long-span precast diaphragms. The strength, stiffness, and ductility of the double tee diaphragms for the cases of topped and pre-topped were investigated. Fleischman et al. [10, 11] conducted research projects about precast concrete diaphragms to establish underlying design philosophy and planned analytical/ experimental activities. Ju and Lin [12] analyzed a total of 520 buildings including rectangular, U-shaped and T-shaped buildings with and without shear walls. The buildings were modeled by both rigid-floor and flexible-floor assumptions. They concluded that the rigid diaphragm assumption was sufficient for buildings without shear walls based on response-spectrum analyses. Whereas, they achieved a large difference between rigid-floor and flexible-floor assumptions for the buildings with shear walls.

Tena-Colunga et al. [13] studied a different type of floor systems such as two-way ribbed RC slabs, beam and block, steel decks and waffle RC flat slabs to investigate the potential flexibility of diaphragm by assessing different plan aspect ratios of the buildings and stiffness of floor systems. They concluded that for office buildings, particularly floor spans greater than 10 m, semi-rigid, semi-flexible or flexible behavior can be observed in floor diaphragms based on performed linear finite element analyses.
Torsional effects on the buildings under earthquake loads are classified as inherent and accidental torsion. Inherent torsion occurs when center of mass (CM) and center of rigidity (CR) do not coincide. While accidental torsion is indirectly considered in earthquake codes by shifting the CM with a constant ratio of floor plan dimensions or applying a torsional moment at the CM corresponding to seismic force multiply by accidental eccentricity. The causes of accidental torsion may be explained as i) the difference between the real and design mass distributions, ii. the variations of the center of rigidity because of unpredictable mechanical properties in seismic force-resisting system, iii. Un-symmetrical yielding of the components of seismic force-resisting system, iv. Torsional ground motion [14].

Fahjan et al. [15] and Xuanhua et al. [16] proposed alternative procedures to account for accidental torsion for response spectrum analysis. Akyürek [17] also recommended a design eccentricity formula including frequency ratio (torsional frequency/ translational frequency) and effective rotational radius. Basu et al. [14], Basu and Giri [18] proposed a method to account for accidental eccentricity via torsional ground motion as a product of accidental eccentricity and translational ground motions.

There are very few studies including accidental eccentricity in semi-rigid diaphragms. Fang [19] investigated the seismic behavior of steel structures with semi-rigid diaphragms. In his study, the distribution of diaphragm forces was assumed as triangular.

In this study, a simple procedure was proposed to account for accidental eccentricity for symmetrical plan framed buildings with a semi-rigid diaphragm to be used in equivalent earthquake load method. The total accidental torsion was defined as the summation of the moment created by fictitious nodal forces which were calculated by multiplying nodal mass with the distance between CM of diaphragm and node coordinate. A single story precast concrete building (RC) consisting of cantilever-type columns tied with pinned connections to roof girders was used as the first numerical example to evaluate the proposed method. The roof consists of corrugated sandwich panels with polyurethane foam core. The poor diaphragm behavior of these buildings was widely reported as one of the main causes of damage and partial collapse [20-28]. A truss model proposed by

Yüksel et al [29] was used for in-plane behavior of the roof panels. The roof was also modeled as the rigid diaphragm and the responses under accidental torsion are compared. As a second numerical example, single story RC building was chosen for the verification of proposed procedure.

2. Proposed Procedure

According to Turkish Building Earthquake Code (TBEC 2018) [30], accidental eccentricity to be used in equivalent seismic load method can be considered as an additional torsional moment applied to CM of the floor diaphragms. These torsional moments are shown in Figure 2 as $M_{ti}^{(X)}$ and $M_{ti}^{(Y)}$ for the loading directions X and Y, respectively.

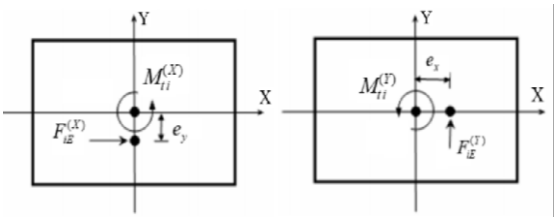

Figure 2. The consideration of accidental eccentricity for equivalent seismic load method

Where, $F_{iE}^{(X)}$ and $F_{iE}^{(Y)}$ are the equivalent seismic loads at i^{th} story for X and Y directions, e_x and e_y are corresponding accidental eccentricities, respectively. Then one can calculate the equivalent torsional moments due to accidental eccentricities as:

$$M_{ti}^{(X)} = F_{iE}^{(X)}\, e_y \qquad M_{ti}^{(Y)} = F_{iE}^{(Y)}\, e_x \tag{1}$$

Consideration of accidental eccentricity as equivalent torsional moments can be applied only when rigid diaphragm assumption is valid. The proposed procedure herein uses the same total torsional moments $M_{ti}^{(X)}$ and $M_{ti}^{(Y)}$. However, the procedure distributes total moments to the frame nodes as fictitious forces based on their tributary mass and rotational inertia. Therefore, accidental eccentricity for semi-rigid diaphragms could be taken into account.

The moment of inertia of a point mass is calculated as the square of the mass times the perpendicular distance to the rotation axis of the joint, $I_0 = m\, r^2$. From this point of view, each nodal mass may oppose to rotational inertia forces mass times the perpendicular distance ($f = m\ r$). Instead of using distance r, accidental torsional moments on the floors may be considered separately for X and Y directional frames. Eq. 2 is given to define this:

$$m_{tj}^{(X)} = f_{tj}^{(X)}\, Y_j \qquad m_{tj}^{(Y)} = f_{tj}^{(Y)}\, X_j \tag{2}$$

Where, $m_{tj}^{(X)}$ and $m_{tj}^{(Y)}$ are the torsional moments calculated by multiplying fictitious nodal forces $f_{tj}^{(X)}$ and $f_{tj}^{(Y)}$ with Y_j and X_j joint coordinates with respect to CM, respectively. These fictitious forces are calculated in the following equations:

$$f_{tj}^{(X)} = \beta^{(X)} m_j\, Y_j \qquad f_{tj}^{(Y)} = \beta^{(Y)} m_j\, X_j \tag{3}$$

Where, m_j is j^{th} node mass, $\beta^{(X)}$ and $\beta^{(Y)}$ are factors calculated from total accidental torsional moments $M_{ti}^{(X)}$ and $M_{ti}^{(Y)}$. The factors are calculated as follows:

$$M_{ti}^{(X)} = \sum_{j=1}^{N} m_{tj}^{(X)} = \sum_{j=1}^{N} f_{tj}^{(X)}\, Y_j = \sum_{j=1}^{N} \beta^{(X)} m_j\, Y_j^2$$

$$\beta^{(X)} = \frac{M_{ti}^{(X)}}{\sum_{j=1}^{N} m_j\, Y_j^2} \tag{4}$$

$$M_{ti}^{(Y)} = \sum_{j=1}^{N} m_{tj}^{(Y)} = \sum_{j=1}^{N} f_{tj}^{(Y)}\, X_j = \sum_{j=1}^{N} \beta^{(Y)} m_j\, X_j^2$$

$$\beta^{(Y)} = \frac{M_{ti}^{(Y)}}{\sum_{j=1}^{N} m_j\, X_j^2} \tag{5}$$

The idealization of a total accidental moment for Y directional seismic load in terms of fictitious nodal forces is shown in Figure 3.

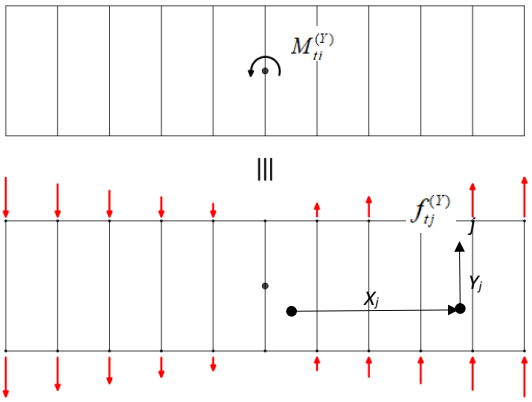

Figure 3. Idealization of torsional moment due to accidental eccentricity

3. Numerical Examples

Single-story precast RC building and single-story RC building were chosen as numerical examples. The step-by-step application of the proposed procedure was presented in the precast example. The RC building example was utilized in order to validate the proposed procedure with SAP2000 program.

3.1. Single-story precast industrial building

A single-story precast industrial building was used to implement the proposed methodology. The front elevation and roof plan are shown in Figure 4 and Figure 5, respectively. The seismic load-resisting system of the building consists of cantilever type columns tied with pinned connections to roof girders. The building plan dimensions are 20×80 m consisting of 1 bay with 20 m length in the X direction and ten bay with 8 m length in the Y direction. The clear length of the columns is 8 m.

The purlins were located at 1.93 m intervals on non-prismatic roof girders. Both of the connections of the roof girder to columns, gutter beams to columns and purlins to roof girders were pinned. The cross-sectional dimensions of the roof girder, purlin, gutter beam, column and RC panel are illustrated in Figure 6. The four sides of the building were covered by RC concrete panels whose connections to the gutter beam are roller and to the ground fixed. Therefore, the panels did not transfer their weight to the structure. However, half of their seismic mass assumed was found at the roof level.

The finite element model (FEM) of the building was created by SAP2000 [31] program and the perspective view is shown in Figure 7. All of the structural members were modeled as frame members. The connections of gutter beams and purlins to roof girders and roof girders to column's gussets were defined as pinned. The roof was covered by corrugated sandwich panels with polyurethane foam core. Truss members were used to model in-plane behavior of the roof panels [29].

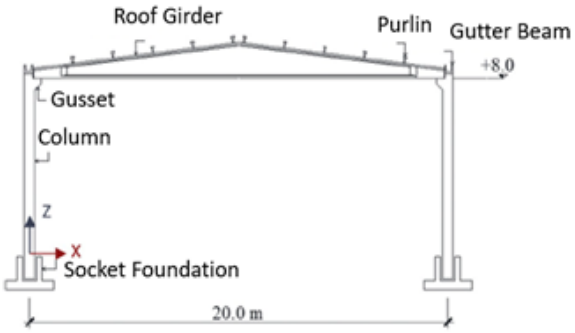

Figure 4. The elevation view of the precast building

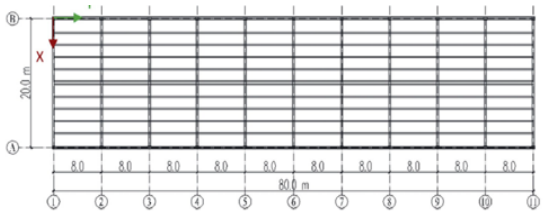

Figure 5. The plan of the precast building

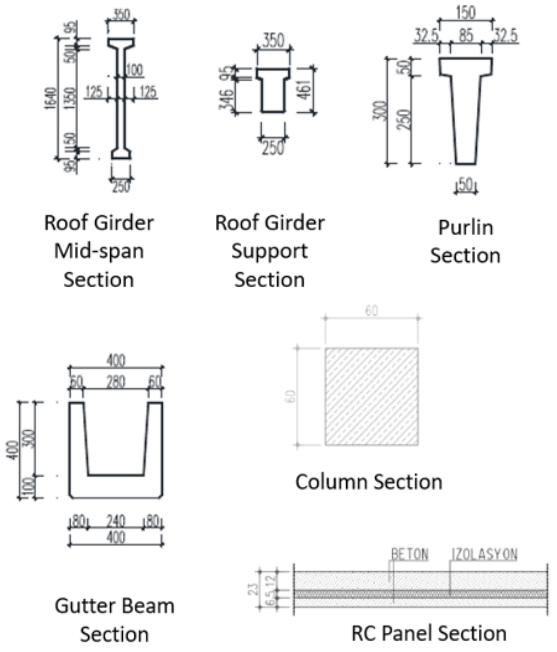

Figure 6. The cross-sectional dimensions of structural elements

3.1.1. Definition of roof diaphragm

The effective stiffness of the truss members was calculated from the following equation [29]:

$$k_{0.01} = \frac{(EA)_e}{L_p} = \frac{\alpha \times \gamma \times (\pi \times D) \times (t_1 + t_2) \times f_y \times n}{0.02 \times L} \quad (6)$$

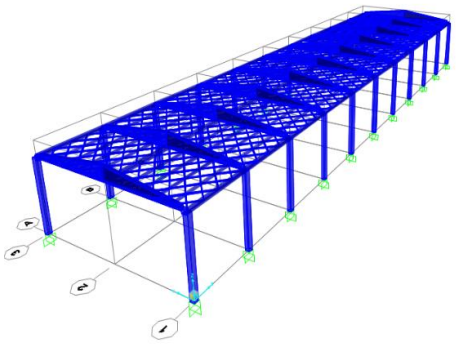

Figure 7. Perspective view of numerical example

Where, L_p is the length of the truss member, α is the effective area of fasteners and is neglected in this study and taken α value of 1, γ is direction factor (safety factor to account for loading direction and experimental uncertainties, the recommended value is 0.67), D is diameter of fasteners, t_1 and t_2 are bottom and top sheet thicknesses, f_y is the yield strength of the sheets, n is number of fasteners per meter, and L is span length of the sandwich panel (the distance between purlins).

The truss members were arranged at 2 m intervals in the Y direction. From geometry, L_p is equal to 2.779 m and corresponding truss angle (θ) was then calculated as 46.02°. The fastener parameters are D=4 mm, $t_1 = t_2$=*0.4 mm*, n =5.5 and f_y =255 MPa. The parameter γ was taken as 0.67. From the above equation, effective stiffness of truss member is calculated as $(EA)_e$ =765225 MPa. Also, the design capacity of the panels is given by:

$$F_{\max} = 0.02 \times (EA)_e \times \cos\theta = 10.6 \text{ kN} \quad (7)$$

3.1.2. Loads and joint masses

The loads applied to building are as follows:

i) *Facade* : 4.50kN/m^2
(only involved in mass calculation)
ii) *Roof covering* : 0.12 kN/m^2
iii) *Snow loading* : 0.75 kN/m^2
iv) *Purlin* : 4.88 kN
(one piece of 8m)
v) *Gutter Beam* : 16.40 kN
(one piece of 8m)
vi) *Roof Beam* : 83.00 kN
(one piece of 19.4 m)

In accordance with TBEC-2018, the masses were calculated from the seismic weight combination of $w_j = w_{G,j} + 0.3 w_{S,j}$ .Where, w_j is j^{th} node seismic weight, $w_{G,j}$ and $w_{S,j}$ are the dead and snow load participation, respectively. Seismic mass for j^{th} node then calculated as $m_j = w_j / g$. The nodal masses were determined as 29.45 kNs^2/m and 26.01 kNs^2/m at inner and outer nodes, respectively. The total mass of the building was calculated as 634.14 kNs^2/m.

3.1.3. Modal analysis

Modal analysis was performed and mode shapes and modal participation mass ratios were calculated. Modal participation mass ratios are listed in Table 1 and the first three vibrational mode shapes are shown in Figure 8-10.

Table 1. Modal participation mass ratios

Mod No	Period (sec)	U_X	U_Y	θ_Z
1	0.892	0.000	0.941	0.000
2	0.891	0.997	0.000	0.000
3	0.877	0.000	0.000	0.882

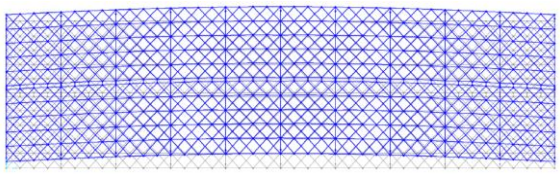

Figure 8. First mode shape, dominant mode in Y direction

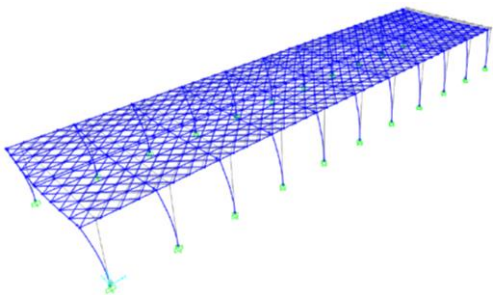

Figure 9. Second mode shape, dominant mode in X direction

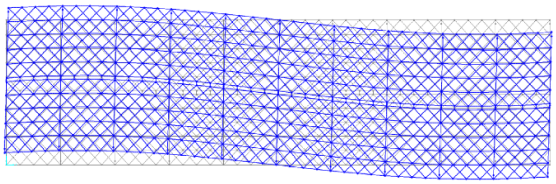

Figure 10. Third Mode Shape, dominant mode in torsional direction

3.1.4. Implementation of equivalent earthquake load method

The building is assumed to be located at latitude 40.871923 and longitude 29.38123 on Z3 local site class. Based on coordinates and soil class, in accordance with TBEC-2018, short period map spectral acceleration coefficient is S_S=1.082, map spectral acceleration coefficient for 1.0 sec is S_1=0.302 and corresponding design acceleration coefficients are S_{DS}=1.298 and S_{D1}=0.453. The elastic design acceleration spectrum then is drawn in Figure 11.

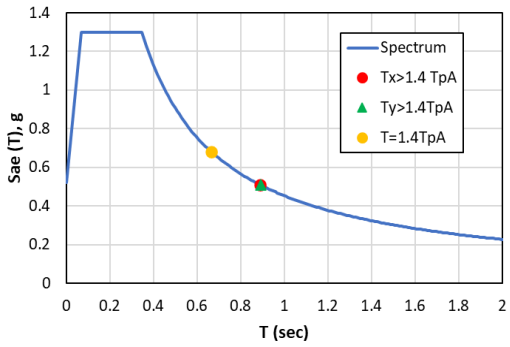

Figure 11. Elastic acceleration design spectrum

Empirical dominant natural vibration period was calculated by following Eq. 8:

$$T_{pA} = C_t H_N^{3/4} = 0.1 \times 8^{3/4} = 0.476 \,\text{sec} \tag{8}$$

TBEC-2018 does not allow a natural period value greater than $1.4T_{pA} = 0.666$ sec. Therefore, equivalent seismic forces should be determined using the empirical period value. The spectral acceleration corresponding to X, Y directional dominant periods together with $1.4T_{pA}$ is also depicted in Figure 11.

The building is classified as single-story building in which seismic loads are fully resisted by columns with hinged upper connections and corresponding seismic behavior factor R=3.0 and overstrength factor D=2.0. As an industrial building, the importance factor was taken as 1.0. Earthquake load reduction factor (R_a) was calculated by the following formula for $T>T_B$:

$$R_a = \frac{R}{I} = \frac{3}{1} = 3 \tag{9}$$

Total seismic base shear was determined from Eq. 10:

$$V_{tE}^{(X)} = m_t S_{aR}\left(T_p^{(X)}\right) \geq 0.04\, m_t I S_{DS} g \tag{10}$$

Where, $S_{aR}\left(T_p^{(X)}\right)$ is reduced design spectral acceleration in terms of g and calculated as:

$$S_{aR}\left(T_p^{(X)}\right) = \frac{S_{ae}\left(T_p^{(X)}\right)}{R_a\left(T_p^{(X)}\right)} \tag{11}$$

Since, semi-rigid diaphragm is assigned to roof plane, equivalent seismic force should be distributed through diaphragm. Herein, the forces were distributed to column top nodes. As a single-story building, the base shear is equal to total of equivalent seismic force. The distribution of equivalent seismic forces to joints were calculated by Eq. 12:

$$f_{jE}^{(X)} = \frac{f_{iE}^{(X)}}{m_i} m_j \qquad f_{jE}^{(Y)} = \frac{f_{iE}^{(Y)}}{m_i} m_j \tag{12}$$

The base shear and the equivalent earthquake load for inner and outer nodes are given in Table 2.

Table 2. Base shears and equivalent nodal earthquake forces

$V_{tE}^{(X)} = V_{tE}^{(Y)}$ (kN)	$V_{tE\_min}^{(X)} = V_{tE\_min}^{(Y)}$ (kN)	$f_{jE}^{(X)} = f_{jE}^{(Y)}$ (kN)	
		Inner Nodes	Outer Nodes
1410.5	323.1	65.5	57.9

The implementation of equivalent earthquake loads for X and Y directions are shown in Figure 12 and Figure 13, respectively.

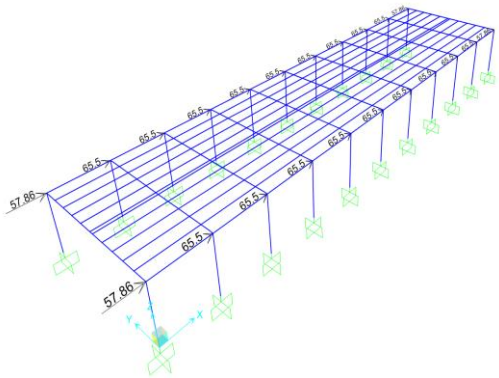

Figure 12. Implementation of equivalent seismic forces for X direction

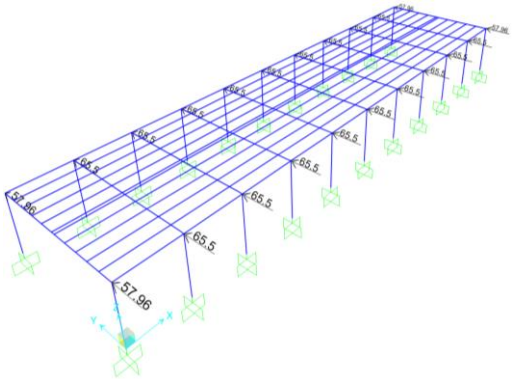

Figure 13. Implementation of equivalent seismic forces for Y direction

3.1.5. Assessment of flexible diaphragm condition

In order to assess the flexible diaphragm condition, the building is opposed to Y directional equivalent seismic forces. The deflected shape including the displacements values at mid-span and corner is shown in Figure 14.

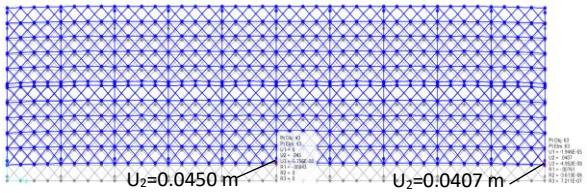

Figure 14. Deflected shape under Y Direction Equivalent Seismic Forces

Since the ratio $\delta_{MDD}/\ \delta_{ADVE}$ = 0.045/0.0407= 1.106<2 the roof can be classified as semi-rigid diaphragm.

3.1.6. Implementation of accidental torsion in terms of fictitious forces

In accordance with TBEC-2018, the accidental eccentricities were taken as 5% of the plan dimensions. The total accidental torsional moments were calculated from Eq. 1 as $M_{ti}^{(X)}$ =1410.5 kNm and $M_{ti}^{(Y)}$=5642.0 kNm. These moments were distributed to nodes as equivalent fictitious forces $f_{tj}^{(X)}$ and $f_{tj}^{(Y)}$.The calculation of the parameters $\beta^{(X)}$ and $\beta^{(Y)}$ using the equations 4 and 5 and corresponding fictitious forces determined from Eq. 3. are listed in Table 3 and Table 4. Implementation of fictitious forces to numerical model for X and Y directions are illustrated in Figure 15 and Figure 16, respectively.

Table 3. Calculation of fictitious forces to account for accidental eccentricity in the X direction

Joint No (j)	m_j (kNs²/m)	Y_j (m)	$\beta^{(X)} m_j Y_j^2$ (kNs²m)	$f_{tj}^{(X)}$ (kN)
1	26.01	-10	2601.3	5.79
2	29.45	-10	2944.8	6.55
3	29.45	-10	2944.8	6.55
4	29.45	-10	2944.8	6.55
5	29.45	-10	2944.8	6.55
6	29.45	-10	2944.8	6.55
7	29.45	-10	2944.8	6.55
8	29.45	-10	2944.8	6.55
9	29.45	-10	2944.8	6.55
10	29.45	-10	2944.8	6.55
11	26.01	-10	2601.3	5.79
12	26.01	10	2601.3	-5.79
13	29.45	10	2944.8	-6.55
14	29.45	10	2944.8	-6.55
15	29.45	10	2944.8	-6.55
16	29.45	10	2944.8	-6.55
17	29.45	10	2944.8	-6.55
18	29.45	10	2944.8	-6.55
19	29.45	10	2944.8	-6.55
20	29.45	10	2944.8	-6.55
21	29.45	10	2944.8	-6.55
22	26.01	10	2601.3	-5.79
		Σ=	**63412.2**	
	$\beta^{(X)}$=		**0.022243**	

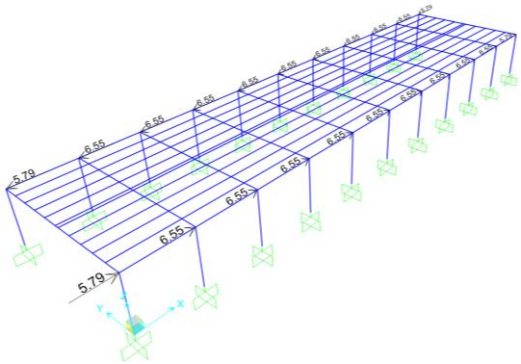

Figure 15. Implementation of accidental torsion in terms of fictitious forces in the X direction

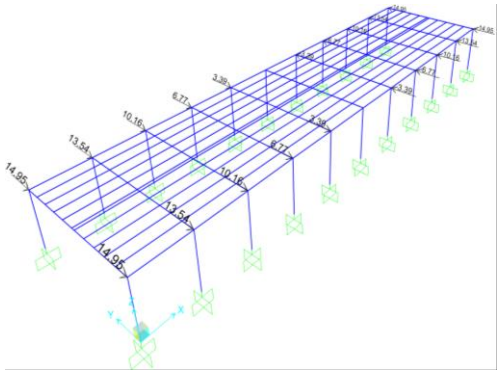

Figure 16. Implementation of accidental torsion in terms of fictitious forces in the Y direction

Table 4. Calculation of fictitious forces to account for accidental eccentricity in the Y direction

Joint No (j)	m_j (kNs²/m)	X_j (m)	$\beta^{(Y)} m_j X_j^2$ (kNs²m)	$f_{tj}^{(Y)}$ (kN)
1	26.01	-40	41620.3	-14.95
2	29.45	-32	30155.2	-13.54
3	29.45	-24	16962.3	-10.16
4	29.45	-16	7538.8	-6.77
5	29.45	-8	1884.7	-3.39
6	29.45	0	0.0	0.00
7	29.45	8	1884.7	3.39
8	29.45	16	7538.8	6.77
9	29.45	24	16962.3	10.16
10	29.45	32	30155.2	13.54
11	26.01	40	41620.3	14.95
12	26.01	-40	41620.3	-14.95
13	29.45	-32	30155.2	-13.54
14	29.45	-24	16962.3	-10.16
15	29.45	-16	7538.8	-6.77
16	29.45	-8	1884.7	-3.39
17	29.45	0	0.0	0.00
18	29.45	8	1884.7	3.39
19	29.45	16	7538.8	6.77
20	29.45	24	16962.3	10.16
21	29.45	32	30155.2	13.54
22	26.01	40	41620.3	14.95
		Σ=	**392645.0**	
		$\beta^{(Y)}$=	**0.014369**	

3.1.7. Deformed shapes under combined forces

Equivalent earthquake forces and fictitious forces due to accidental torsion are combined as depicted for two cases: i. Positive X directional forces and counter-clockwise torsional direction ii. Positive Y directional forces and counter-clockwise torsional direction. These loading are shown in Figure 17.

Under combined forces +EXP and +EYP, the deformed shapes are drawn in Figures 18 and 19, respectively.

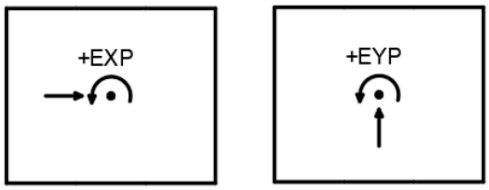

Figure 17. Combination of equivalent earthquake forces with accidental torsion

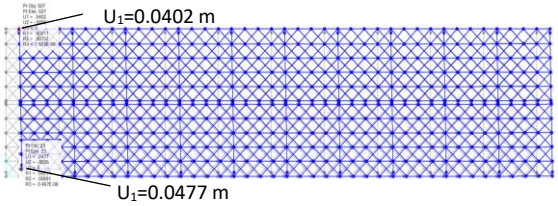

Figure 18. The deformed shape under loading +EXP (semi-rigid diaphragm)

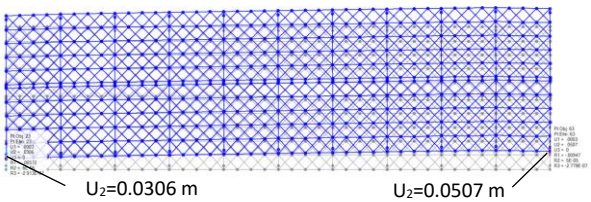

Figure 19. The deformed shape under loading +EYP (semi-rigid diaphragm)

3.1.8. Modeling of the building with rigid diaphragm

The structure was also modeled with rigid diaphragm (Figure 20). Equivalent seismic forces and accidental moments were applied to the master joint located on CM of diaphragm for X and Y directions. Since the connections of the columns to the main girder and gutter beams are pinned, the free vibration periods are the same as the building modeling by a semi-rigid diaphragm. Hence, the loads applied are the same for both models. The deflected shapes under +EXP and +EYP loading are shown in Figure 21 and Figure 22, respectively.

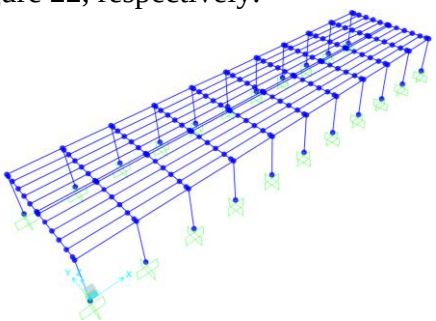

Figure 20. The numerical model with rigid diaphragm

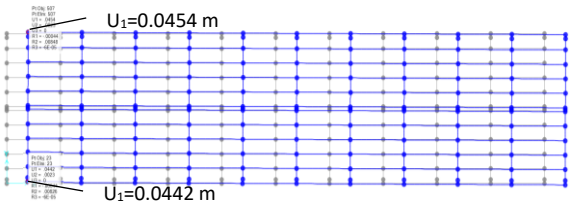

Figure 21. Deformed Shape under loading +EXP (rigid diaphragm assumption)

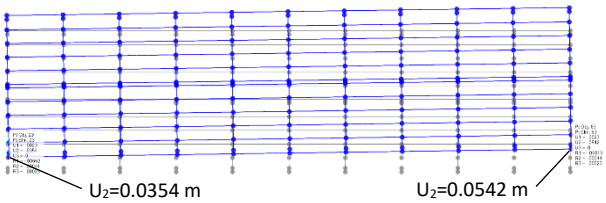

Figure 22. Deformed Shape under loading +EYP (rigid diaphragm assumption)

3.1.9. Comparison of rigid and semi-rigid diaphragm assumptions in terms of displacements

The maximum and minimum reduced drifts (Δ_{max}) and (Δ_{min}) were calculated for the two types of diaphragm modeling approaches and given in Table 4 and Table 5. In addition, the torsional irregularity coefficients (η_{bi}) for rigid and semi rigid diaphragm cases can be found in Table 5 and Table 6 for X and Y direction, respectively. According to TBEC-2018, η_{bi} is calculated from the following equation.

$$\eta_{bi} = \frac{\Delta_{i\max}}{\Delta_{iave}} \qquad \Delta_{iave} = \frac{\Delta_{i\max} + \Delta_{i\min}}{2} \tag{11}$$

Table 5. Comparison of the displacements obtained from rigid and semi-rigid diaphragm modeling approaches for X direction

Diaphragm Type	X Direction		
	Δ_{max} (m)	Δ_{min} (m)	η_{bi}
Semi-rigid	0.0477	0.0402	1.085
Rigid	0.0454	0.0442	1.013

Table 6. Comparison of the displacements obtained from rigid and semi-rigid diaphragm modeling approaches for Y direction

Diaphragm Type	Y Direction		
	Δ_{max} (m)	Δ_{min} (m)	η_{bi}
Semi-rigid	0.0507	0.0306	1.247
Rigid	0.0542	0.0354	1.210

3.2. Single story reinforced concrete building

3.2.1. The geometry of the building

Second numerical example is single story RC building (Figure 23). The bay widths in X direction were equally spaced as 8 m and the bay width in Y direction was 10m. The column cross-sectional dimensions were selected as 50×150 cm and 50×50 cm at the corner and inner columns, respectively to increase the diaphragm flexibility of the building. Also, the slabs were divided into1.0m x 1.0m meshes to account for mass distribution. The cross-sectional dimension of beam was 30×60 cm. The building height was 8 m and the slab thickness was 25 cm. Column, beam and slab weights were automatically calculated by the program. Effective rigidity values were assigned for columns, beams and slabs' cross sections in accordance with TBEC-2018.

3.2.2. The loads, seismic masses, earthquake design parameters

Covering and live loads were taken as 2 kN/m^2 and 5 kN/m^2, respectively. The same spectral parameters with numerical example 1 were used in equivalent earthquake load method. The definitions in TBDY-2018, total mass and base shear values for Y direction are listed in Table 7. Since the diaphragm flexibility effects are significant for Y direction, the analysis results are only be discussed for Y direction. Semi-rigid diaphragm was assigned to the nodes at 8 m level. Mass values were calculated automatically for each joint based on their tributary areas in FEM. The program converts the seismic weight calculated from g+nq loading to joint masses. Then equivalent seismic story forces were contributed to the joints proportional to their masses.

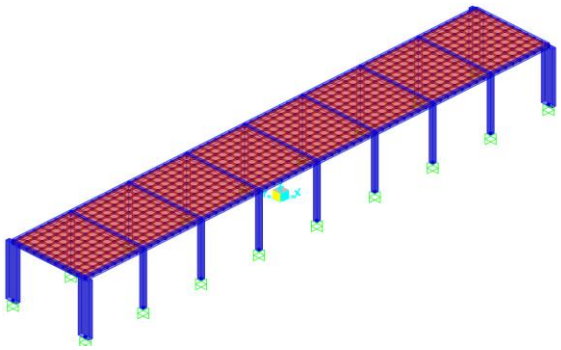

Figure 23. Perspective view of RC Building

Table 7. Parameters to be used in the equivalent seismic load method

Parameter	Value
Building Importance Factor (I)	1
Building Occupancy Class (BKS)	3
Earthquake Design Class (DTS)	1
Building Height Class (BYS)	7
Building Behavior Factor (R)	8
Overstrength Factor (D)	3.0
Total Seismic Mass (m_t)	772.8 kNs^2/m
Vibration period in Y direction	0.662 sn
Base Shear Force in Y Direction	647.05 kN

3.2.3. Assessment of flexible diaphragm condition

The equivalent seismic force method without accidental eccentricity was implemented to the building in Y direction to check for flexible diaphragm condition (Figure 24). The mid-span and corner displacements are depicted in a deformed shape in Figure 24. Since $\delta_{MDD}/\delta_{ADVE}$ =0.0105/0.0067=1.567 was between 1 and 2, diaphragm can be classified as semi-rigid.

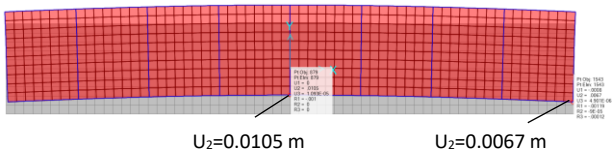

Figure 24. Deflected Shape under Y Direction Equivalent Seismic Forces

3.2.4. Verification of proposed methodology

The accidental eccentricity effects were evaluated using two different ways in order to verify the proposed methodology. The first way was to use automated algorithm in FEM which automatically distributes accidental eccentricity effects to nodes. The second way was using the proposed methodology. As applied in Example 1, the total accidental torsion was contributed to nodal fictive forces proportional to joint masses and coordinates. Figure 25 depicts the implementation of the proposed procedure for Y direction and the deflected shape for +EYP loading is shown in Figure 26.

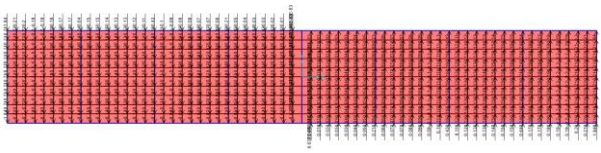

Figure 25. Implementation of accidental torsion in terms of fictitious forces in Y direction

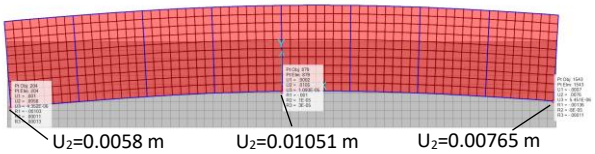

Figure 26. The deformed shape under loading +EYP (semi-rigid diaphragm)

The calculated reduced drift values obtained from FEM automated procedure and proposed methodology are listed in Table 8. The left and right corner displacements are Δ_{min} and Δ_{max} are given together with Δ_{MDD}. As it is seen, the results are very close to each other.

Table 8. Comparison of the displacements obtained from proposed and FEM automated procedures for Y direction

Procedure for accidental eccentricity	Y Direction		
	Δ_{max} (m)	Δ_{MDD} (m)	Δ_{min} (m)
Automated procedure built in FEM	0.00763	0.01051	0.00581
Proposed	0.00765	0.01051	0.00580

4. Conclusions

A simple numerical procedure was proposed to account for the accidental eccentricity effects on the symmetrical frame-type buildings having semi-rigid diaphragms. Two numerical examples, which are single-story RC precast building and single-story RC building, were implemented for the proposed procedure.

Single Story RC Precast Building

The building was modeled with semi-rigid and rigid diaphragm assumptions to investigate the behavior difference between the buildings. The following conclusions can be drawn from this case:

1) The maximum reduced displacement demands obtained from the building with semi-rigid diaphragm were 5.07% greater and 6.55% smaller than those obtained with rigid diaphragm assumptions, for X and Y directions, respectively.

2) Greater torsional irregularity factors were obtained of 7.11% and 3.06% from building with semi-rigid diaphragm for X and Y directions, respectively.

3) This shows the significance of considering accidental eccentricity effects on semi-rigid diaphragms to safely design the buildings.

Single-Story RC Building

Single-story RC building was chosen to verify the proposed procedure with FEM built-in algorithm. The building was modeled by semi-rigid diaphragm in the software. The proposed and automated procedures were compared in terms of displacements obtained. The results were well correlated.

It is concluded from this study that the proposed methodology is reliable and can be used for modeling accidental eccentricity effects on symmetrical-plan buildings with semi-rigid diaphragms.

Article Information Form

Acknowledgments
The author would like to thank Prof. Dr. Ercan Yüksel for his contributions to the paper.

Funding
The author has not received any financial support for the research, authorship, or publication of this study.

The Declaration of Conflict of Interest/ Common Interest
No conflict of interest or common interest has been declared by the author.

The Declaration of Ethics Committee Approval
This study does not require ethics committee permission or any special permission.

The Declaration of Research and Publication Ethics
The author of the paper declares that they comply with the scientific, ethical and quotation rules of SAUJS in all processes of the paper and that they do not make any falsification on the data collected. In addition, they declare that Sakarya University Journal of Science and its editorial board have no responsibility for any ethical violations that may be encountered, and that this study has not been evaluated in any academic publication environment other than Sakarya University Journal of Science.

References

[1] ASCE-7, "Minimum design loads for buildings and other structures. ASCE standard ASCE/SEI 7-16," American Society of Civil Engineering, ISBN 0-7844-7996-4, 2016.

[2] P. Mortazavi, J. Humar, "Consideration of diaphragm flexibility in the seismic design of one-story buildings," Engineering Structures, vol. 127, pp. 748-758, 2016.

[3] J. Humar, M. Popovski, "Seismic response of single-storey buildings with flexible diaphragm," Canadian Journal of Civil Engineering, vol. 40, pp. 875-886, 2013.

[4] V. K. Sadashiva, G. A. MacRae, B. L. Deam, "A Mechanics Based Approach to Quantify Diaphragm Flexibility Effects," Proceedings of the Ninth Pacific Conference on Earthquake Engineering Building an Earthquake-Resilient Society, Auckland, New Zealand, 2011, pp. 114-121.

[5] V. K. Sadashiva, G. A. MacRae, B. L. Deam, M. S. Spooner, "Quantifying the seismic response of structures with flexible diaphragms," Earthquake Engineering and Structural Dynamics, vol. 41, pp. 1365-1389, 2012.

[6] R. Tremblay, T. Berair, A. Filiatrault, "Experimental Behaviour of Low-Rise Steel Buildings with Flexible Roof Diaphragms," 12th World Conference on Earthquake Engineering, Auckland, New Zealand, 2000, pp. 2567-2575.

[7] K. M. Shrestha, "Use of flexible and ductile roof diaphragms in the seismic design of single-storey steel buildings," Doctor of Philosophy McGill University, 2011.

[8] K. T. Farrow, R. B. Fleischman, "Effect of Dimension and Detail on the Capacity of Precast Concrete Parking Structure Diaphragms," PCI Journal, vol. 48, no.5, pp. 46-61, 2003.

[9] R. B. Fleischman, K. T. Farrow, "Seismic Design Recommendations for Precast Concrete Diaphragms in Long Floor Span Construction," PCI Journal, vol. 48, no.6, pp. 46-62, 2003.

[10] R. B. Fleischman, C. J. Naito, J. Restrepo, R. Sause, S. K. Ghosh, "Seismic Design Methodology for Precast Concrete Diaphragms Part 1: Design Framework," PCI Journal, vol. 50, no.5, pp. 68-83, 2005.

[11] R. B. Fleischman, S. K. Ghosh, C. J. Naito, G. Wan, J. Restrepo, M. Schoettler, R. Sause, L. Cao, "Seismic Design Methodology for Precast Concrete Diaphragms Part 2: Design Framework," PCI Journal, vol. 50, no. 6, pp. 14-31, 2005.

[12] S. H. Ju, M.C. Lin, "Comparison of Building Analyses Assuming Rigid or Flexible Floors," Journal of Structural Engineering, vol. 125, no. 1, pp. 25-31, 1999.

[13] A. Tena-Colunga, K. L. Chinchilla-Portillo, G. Juarez-Luna "Assessment of the diaphragm condition for floor systems used in urban buildings," Engineering Structures, vol. 93, pp. 70-84, 2015.

[14] D. Basu, M. C. Constantinou, A. S. Whittaker, "An equivalent accidental eccentricity to account for the effects of torsional ground motion on structures," Engineering Structures, vol. 69, pp. 1-11, 2014.

[15] Y. M. Fahjan, C. Tüzün, J. Kubin, "An Alternative Procedure for Accidental Eccentricity in Dynamic Modal Analyses of Buildings," First European Conference on Earthquake Engineering and Seismology, Genewa, Switzerland, 2006, pp. 1166-1174.

[16] F. Xuanhua, Y. Jiacong, S. Shuli, C. Pu, "An alternative approach for computing seismic response with accidental eccentricity," Earthquake Engineering and Engineering Vibration, vol. 13, pp. 401-410, 2014.

[17] O. Akyürek, "Tasarım eksatrikliği için alternatif bir öneri," Journal of Polytechnic, vol. 26, no. 2, pp. 609-623, 2023.

[18] D. Basu, S. Giri, "Accidental eccentricity in multistory buildings due to torsional ground motion," Bulletin of Earthquake Engineering, vol. 13, pp. 3779-3808, 2015.

[19] C. Fang, "The Seismic Behavior of Steel Structures with Semi-Rigid Diaphragms," Doctor of Philosophy Virginia Ploytechnic Institute and State University, 2015.

[20] Ş. Özden, H. Erdoğan, E. Akpınar, H. M. Atalay, "Performance of precast concrete structures in October 2011 Van earthquake, Türkiye," Magazine of Concrete Research, vol. 66, no. 11, pp. 543-552, 2014.

[21] M. Fishinger, B. Zoubek, T. Isakovic, "Seismic Response of Precast Industrial Buildings," Perspectives on European Earthquake Engineering and Seismology, vol. 1, pp. 131-177, 2015.

[22] A. Belleri, E. Brunesi, R. Nascimbene, M. Pagani, P. Riva, "Seismic Performance of Precast Industrial Facilities Following Major Earthquakes in the Italian Territory," Journal of Performance of Constructed Facilities, vol. 29, no. 5, pp. 1-10, 2014.

[23] M. Saatçioğlu, D. Mitchell, R. Tinawi, N. J. Gardner, "The August 17, 1999, Kocaeli (Türkiye) earthquake - Damage to structures," Canadian journal of Civil Engineering, vol. 28, pp. 715-737, 2001.

[24] M. H. Arslan, H. H. Korkmaz, F. G. Gülay, "Damage and failure pattern of prefabricated structures after major earthquakes in Türkiye and shortfalls of the Turkish Earthquake code," Engineering Failure Analysis, vol. 13, pp. 537-557, 2006.

[25] J. K. Iverson, N. M. Hawkins, "Performance of precast/prestressed concrete building structures during the Northridge earthquake," PCI Journal, vol. 39, no. 2, pp.38-55, 1994.

[26] J. K. Ghosh, N. Cleland, "Observations from the February 27, 2010, earthquake in Chile," PCI Reconnaissance Team Report, PCI Journal, vol. 57, no.1 pp. 52-75, 2012.

[27] S. L. Wood, "Seismic rehabilitation of low-rise precast industrial buildings in Türkiye," In Advances in Earthquake Engineering for Urban Risk Reduction, Springer, Dordrecht, Netherlands, NATO science series IV, vol. 66, Earth and Environmental Sciences, 2003, pp. 167–177.

[28] G. Toniolo, A. Colombo, "Precast concrete structures: the lessons learned from the L'Aquila earthquake," Structural Concrete, vol. 13, pp. 73–83, 2012.

[29] E. Yüksel, A. Güllü, H. Özkaynak, C. Soydan, A. Khajehdehi, E. Şenol, A. M. Saghayesh, H. Saruhan, "Experimental investigation and pseudoelastic truss model for in-plane behavior of corrugated sandwich panels with polyurethane foam core," Structures, vol. 29, pp. 823–842, 2021.

[30] TBEC-2018, "Turkish Building Earthquake Code," Turkish Disaster and Emergency Management Presidency, Türkiye- Lagal Gazette No:30364, Ankara, 2018.

[31] CSI SAP2000 v22.2.0, "Integrated Software for Structural Analysis and Design," Computers and Structures Inc., Berkeley, California, 2020.